Pulses and global bifurcations in a nonlocal reaction-diffusion system

Michael D. Graham*
Department of Chemical Engineering, Princeton University, Princeton, New Jersey 08544-5263

Usuf Middya and Dan Luss
Department of Chemical Engineering, University of Houston, Houston, Texas 77204-4792
(Received 23 April 1993)

Experiments and simulations of simple reaction-diffusion systems in bounded domains with spatially nonlocal coupling display interesting pulse motions that are absent without the nonlocal effect. These include pulses that stick to the boundaries, "bounce" off them, or disappear at one boundary and reappear at the other, as if the domain was periodic. We numerically show that, for a two-variable model system, the transitions between these motions occur through global bifurcations. The transition from a wall-bound stationary front to a "back-and-forth" moving (bouncing) pulse occurs through a symmetric crisis. This motion evolves into a "unidirectional" motion, in which a pulse disappears at one boundary as a new one is born at the other, through a gluing bifurcation. The relationship between the spatiotemporal behavior and its phase-space representation is shown, as well as the importance of the nonlocal effect in creating the required global phase-space structure.

PACS number(s): 82.20.Wt, 05.45.+b, 05.70.Ln

I. INTRODUCTION

The dynamics of stationary and traveling fronts and pulses in reaction-diffusion systems are of interest in many fields. Models of the form

$$\frac{\partial u}{\partial t} = D\nabla^2 u + f(u) \tag{1}$$

have been studied extensively, where $u \in \mathbb{R}^n$ is a vector of concentrations and $D \in \mathbb{R}^n \times \mathbb{R}^n$ is a diagonal matrix of diffusion coefficients. Models of this form include the (real) Ginzburg-Landau equation and the activator-inhibitor models of biological and chemical pattern formation. Coullet and Iooss [1] summarize the local bifurcation theory of stationary spatially periodic solutions to Eq. (1) in one dimension in an unbounded or periodic domain. Elezgaray and Arneodo [2,3] study a two-variable model of this form, with Dirichlet boundary conditions, to explore the possible behavior of the Couette flow reactor [4]. In particular they observe a global bifurcation (crisis) induced by competition between the inherent tendency for the system to "ignite" and the "extinguished" state enforced at the boundaries. The temporal behavior is complex, but the spatial behavior is relatively simple, with no propagating patterns. These studies and most others are limited to cases where the underlying phenomena are spatially local and also generally to periodic or infinite domains. Results such as these may not be valid when spatially *nonlocal* effects are important. In such cases Eq. (1) must be modified to read

$$\frac{\partial u}{\partial t} = D\nabla^2 u + f\left(u, \int h(u(x))dx\right). \tag{2}$$

The subject of this work is the dynamics of fronts and propagating pulses in a nonlocal model and the global bifurcations underlying the dynamics. Nonlocal phenomena arise directly in numerous applications, including spatially extended nonlinear current systems [5–7], ferromagnetic systems [5] and heterogeneous catalytic and electrochemical problems [8–21]. They also arise indirectly when considering the nonlinear interactions of waves traveling in opposite directions in systems whose behavior is, strictly speaking, local [22,23]. Finally, they arise in strictly local models for which some components have very large characteristic length scales, either through very rapid diffusion of the components or slow reaction.

In heterogeneous catalytic systems, the motivation for this work, nonlocal effects arise in two ways. Catalytic wires or ribbons in a flowing reactive gas stream are used in many studies of catalytic processes. These can be electrically heated to control, for example, the average temperature of the ribbon. This mode of control introduces a nonlocal effect into the dynamics, as a change in current changes the resistive heating of the entire ribbon [10,14,16]. The model studied here is an idealization of such an experiment. In other studies, a catalyst is placed in a well-mixed reactor [8,20,21]. The mixing in the gas phase is much faster than transport on the surface, so fluctuations at one point on the surface are communicated rapidly to the entire surface through the gas phase. Thus surface elements are globally coupled.

In a typical (local) excitable reaction-diffusion system in a bounded domain, a pulse generally vanishes upon reaching a boundary and the system relaxes to the ground state. In the system we consider, this behavior is forbidden, as the average "temperature" in the domain is kept constant by a controller. Since a pulse, once formed, is forbidden from leaving the domain, intuitively we expect that it will either stick to the boundary, bounce

off the boundary, or vanish as the temperature increases elsewhere in the domain to maintain a constant average value. All of these possibilities are indeed observed in the simulations; the transitions between these different behaviors form the subject of this work.

In particular, we consider two transitions in a model of a catalytic ribbon: (i) a transition from a stationary front to a traveling pulse that "bounces" back and forth from boundary to boundary [Figs. 1(a)–1(c) and 2(a)]; (ii) a transition from this motion to a "unidirectional" pulse that travels until it reaches a wall, where it disappears while another traveling pulse is born at the opposite wall [Figs. 2(a)–2(d)]. In this pattern, each succeeding pulse travels in the same direction, so the pattern appears very similar to a simple traveling pulse in a periodic domain. Back-and-forth temperature pulses are observed experimentally on a catalytic ribbon [16] and both back-and-forth and unidirectional patterns are found as the result of current instabilities in a dc gas discharge [7]. Neither transition is covered by the local bifurcation scenarios of Coullet and Iooss [1] and we show that they occur through global bifurcations. The first transition occurs through a symmetric crisis [24,25]. The second is a gluing bifurcation, an interaction between two symmetric heteroclinic cycles [26,27]. The correspondence between the phase space and physical (spatiotemporal) behavior is clarified and the role of the nonlocality in the formation of these patterns and transitions is discussed.

II. MODEL

The results we present are solutions to a model that is motivated by studies of the atmospheric pressure oxidation of a chemical species on an electrically heated ribbon of a catalytic metal in a flow reactor [8–19,28,29]. Surface temperature (T) is a fast, autocatalytic variable and the surface catalytic activity (θ) is a slow, nondiffusing

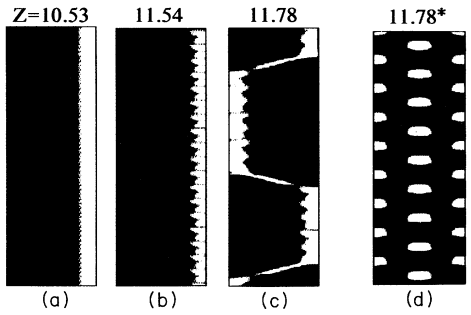

FIG. 1. Stationary to back-and-forth transition. The horizontal axis is position, vertical is time. Black signifies low temperature, white is high. (a) Stationary front; (b) oscillatory front; (c) chaotic back-and-forth motion; (d) unstable symmetric antiphase motion. The asterisk indicates that reflection symmetry was enforced. Because of symmetry, the left and right halves of this pattern individually satisfy the equations and boundary conditions in a domain of half the length shown (i.e., $Z = 5.89$).

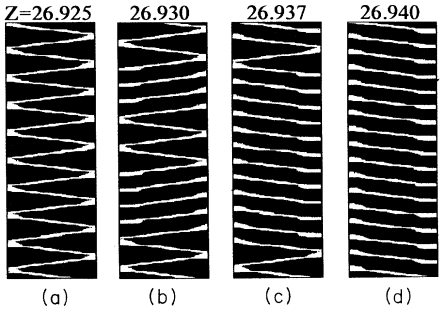

FIG. 2. Back-and-forth to unidirectional transition: (a) periodic back-and-forth motion; (b) and (c) intermediate patterns; (d) unidirectional motion.

variable. The ratio between the kinetic time scales for T and θ is ϵ, and typically is small. The model is [28,29]

$$\epsilon\frac{\partial T}{\partial t} - \nabla^2 T = f(T,\theta;I) \equiv \Gamma(T,\theta) - \eta\left[1+\beta(T-\hat{T})\right](T-T_0) + I^2\left[1+\alpha(T-\hat{T})\right], \tag{3a}$$

$$\frac{d\theta}{dt} = g(T,\theta) \equiv \exp\left[-E_d(T^{-1}-\hat{T}^{-1})\right]\Gamma(T,\theta) - K_a(1-\theta)\exp(-E_a/T), \tag{3b}$$

$$\frac{\partial T}{\partial z} = 0, \quad z = 0, Z, \tag{3c}$$

$$\Gamma(T,\theta) = \frac{\theta}{\theta + K_c\exp(E/T)}. \tag{3d}$$

The nullcline $f(T,\theta;I) = 0$ is S shaped for typical values of electric current I, while the nullcline $g(T,\theta) = 0$ is single valued but nonlinear. The dimensionless length Z is the distinguished parameter in this study. Other parameter values are fixed at $\epsilon = 0.0295$, $K_a = 17.08$, $\alpha = 0.5482$, $\beta = 0.371$, $\eta = 1.84$, $K_c = 1.9 \times 10^{-15}$, $E = 71.53$, $E_a = 44.71$, $E_d = 13.41$, $T_s = 2.000$, $T_0 = 1.097$, and $\hat{T} = 1.974$. Details of the motivation and formulation of the model are given in Refs. [28] and [29].

In the case of fixed current and spatial uniformity, the dynamics occur on the (T,θ) phase plane. The steady states are the intersections of the nullclines $f(T,\theta;I) = 0$ and $g(T,\theta) = 0$. Depending on I and K_a, there are one or three steady states. When $\epsilon \to 0$ the steady states on the upper ("ignited") and lower ("extinguished") branches of $f = 0$ are stable, while those on the intermediate branch are unstable. A limit cycle (relaxation oscillation) is obtained when the unique steady state is unstable. Depending on the values of I and K_a, the system can be classified in the usual way as excitable (E), oscillatory (O), or bistable (B). A narrow parameter range also exists where three steady states exist, but only one is stable (B'). The saddle-node bifurcation that separates B' and O regimes leads directly from a stable steady state to a stable relaxation oscillation through a so-called global

saddle-node bifurcation [30,31].

The full spatiotemporal behavior, of course, does not occur on the phase plane. Relaxing the restriction of spatial uniformity, but keeping I fixed, this model is essentially similar to the classical FitzHugh-Nagumo equations for nerve impulse transmission. However, if the average temperature of the ribbon is fixed (by controlling the ribbon's overall electrical resistance), the current is determined by the integral constraint:

$$\frac{1}{Z}\int_0^Z T(z)dz = T_s. \tag{4}$$

Integration of Eq. (3a) over the domain and application of (3c) and (4) leads to an explicit expression for the current I as a *functional* of T and θ. Substitution of the result into Eq. (3a) yields an integro-differential model in the form of Eq. (2). When the integral constraint is applied, the phase plane classification is only an instantaneous one, as the current is no longer fixed. The transitions we discuss here occur in a range of K_a values near the upper edge of the regime in which O behavior can arise [29].

The nonlocal effect induced by the constraint, Eq. (4), is desynchronizing; an increase in temperature at one point on the surface increases the electrical resistance of the ribbon. In response, the control decreases the current passing through the ribbon, thus decreasing the temperature elsewhere on the catalyst surface. The desynchronizing nonlocal mechanism changes the stability characteristics of the system with respect to uniform (wave number zero) fluctuations [5]. This result is expected intuitively, as a uniform fluctuation demands synchronized behavior of distant surface elements, while the nonlocal effect works against this type of behavior. Conversely, sinusoidal perturbations are permitted, as their leading order effect on the resistance is nil. The present system is most susceptible to long-wavelength perturbations. Thus, because uniform fluctuations are inhibited, the most unstable wave number is unity. In addition, the nonlocal effect accounts for the stability of the traveling pulses observed below, as growth in the size of a hot region on the ribbon decreases the current, inhibiting further growth.

The computations use finite differences for spatial discretization and a semi-implicit Runge-Kutta method for time discretization. Parameter continuation [32] is used to compute unstable solutions and the eigenvalues and eigenfunctions of their linearizations. Thus unstable states that contribute to global phenomena can be identified.

III. TRANSITION FROM STATIONARY FRONT TO TRAVELING PULSE

In an infinite or periodic domain, the transition from a stationary spatially periodic pattern of pulses to a traveling one occurs through a local infinite period bifurcation, which breaks the time invariance and reflection symmetry of the pattern [1]. The boundaries forbid such a transition here and the birth of a traveling pulse is much more complex. Note that the phase plane characterization is bistable for the entire current range encountered during this transition. For relatively small Z, a stable stationary front exists near a wall [Fig. 1(a)]. By reflection symmetry, there are two such solutions; the hot region is either at the left wall or the right. (These solutions are born at a pitchfork bifurcation at $Z = 7.69$.) A pulse initiated anywhere in the domain will travel to one wall or the other and "stick" there, evolving into one of these two stationary solutions. As Z increases above $Z = 10.76$, a Hopf bifurcation [leading to Fig. 1(b)] followed by a period-doubling cascade transforms the stable stationary front into a chaotic attractor. The position of the front changes irregularly, but the hot region is still localized. For slightly larger Z, the localized pattern persists for a time, then "escapes" from the wall in the form of a traveling pulse. The pulse travels to the other wall, oscillates irregularly for a while, then escapes back [Fig. 1(c)]. The process repeats indefinitely, but the time between escapes varies. The time average of the chaotic pattern is reflection symmetric. As the length increases further, the motion becomes more regular and eventually evolves into a periodic "back-and forth" traveling pulse that appears to bounce off the boundaries [Fig. 2(a)].

Figure 3(a) shows a time-delay reconstruction of $T_R - T_L$ for the chaotic attractor of Fig. 1(c), where T_R and T_L are the temperatures at the right and left boundaries. The knots at the lower left and upper right are the intervals of chaotic, but localized front motion. The large excursions correspond to traveling pulses. The attractor is clearly symmetric (invariant under rotation by π in this projection), in accordance with the reflection symmetry of the time-averaged spatial pattern, and approaches a saddle point at the origin, indicating the proximity to a crisis. The two asymmetric chaotic attractors formed by

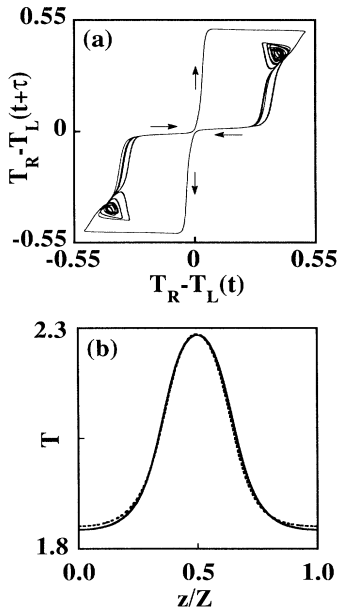

FIG. 3. (a) Time-delay reconstruction of $T_R - T_L$ for the chaotic pattern of Fig. 1(c); (b) instantaneous temperature profiles from Figs. 1(c) (dashed) and 1(d) (solid) at the point of closest approach to one another.

the period-doubling cascade have collided with the stable manifold of a reflection symmetric pattern to form a symmetric attractor [24,25]. Underlying this behavior is a homoclinic bifurcation involving the symmetric saddle point. This saddle point is in fact a reflection symmetric limit cycle, an "antiphase oscillation" [Fig. 1(d)] born at a subcritical Hopf bifurcation at $Z = 12.41$. Figure 3(b) shows instantaneous temperature profiles at the closest approach of the antiphase and traveling pulse motions, clearly showing their proximity. Presumably, even closer to the actual crisis a pulse should approach the center of the domain, then undergo antiphase oscillation for some time before returning to the wall. This has not been observed, because the entire transition, including the period-doubling cascade, takes place in a very narrow interval in Z.

As mentioned in the Introduction, pulses in local reaction-diffusion equations typically disappear at boundaries, unlike the bouncing pulses found above. However, one *atypical* example, due to Tuckwell [33], is worth mentioning, because it does produce bouncing pulses like those in Fig. 2(a), and does so through a mechanism similar to that of the present nonlocal system. In the above results, as a pulse approaches a boundary and the ignited region begins to shrink, the electric current spikes upward to compensate, preventing extinction of the pulse. Tuckwell proposed a local model that is "rigged" such that if two pulses approach each other (equivalent by symmetry to a pulse approaching a no-flux wall), a "boost" is given to the reaction terms, preventing the colliding pulses from relaxing to the ground state. Instead, they bounce, just as we observed above. Tuckwell did not provide a physical motivation for the boost in the reaction terms in his model, but the effect arises naturally in systems with desynchonizing nonlocal coupling.

IV. BACK-AND-FORTH TO UNIDIRECTIONAL TRANSITION

The back-and-forth motion persists until $Z \simeq 26.9$, above which the transition to unidirectional pulses occurs. The transition is not sharp, but occurs via a sequence of intermediate states that are found in a very narrow range of Z [Figs. 2(a)–2(d)]. These states can be represented by sequences of symbols L and R, determined by the boundaries at which successive pulses originate. We denote the back-and-forth motion by $\ldots LRLRLR\ldots = \overline{LR}$ or $\overline{RL}$ and the unidirectional motion of pulses originating at the left (right) boundary by $\ldots LLLL\ldots = \overline{L}$ ($\ldots RRRR\ldots = \overline{R}$). In the transition regime, a periodic or nonperiodic sequence is found, depending on the parameters [Figs. 2(b) and 2(c)]. As above, global bifurcation phenomena are responsible for this complexity.

From Fig. 2, it appears that the only fixed points approached by the back-and-forth and unidirectional trajectories are the stationary fronts [shown in Fig. 1(a), but unstable at the values of Z considered in this section]. Consider the possibility that there are nearly heteroclinic paths connecting one to the neighborhood of the other. One obvious possibility is the traveling pulse motion, which clearly begins with a hot region at one end of the domain and ends with a hot region at the other. Another possibility arises when considering the family of antiphase oscillations, one of which was introduced in Fig. 1(d). Note that because of its symmetry, Fig. 1(d) actually satisfies Neumann boundary conditions in the center of the domain. Thus the pattern corresponding to the left (or right) half of Fig. 1(d) satisfies the governing equations and boundary conditions in a domain of half the length, i.e., $Z = 5.89$. During each half of the oscillation, the pattern appears to approach one or the other of the stationary front solutions, suggesting the possibility that the oscillation eventually becomes heteroclinic. However, the antiphase oscillation becomes unstable at a pitchfork bifurcation at around $Z = 8.65$ and continuation studies were not convergent, so we are unable to directly confirm this possibility, though further evidence for it appears below.

Whether the putative (nearly) heteroclinic paths are actually followed can be determined by studying the actual trajectories that start near one of the front solutions. These patterns, though unstable, can be computed by continuation. For parameters in the transition region, the linearization around the front solution has two real positive eigenvalues; these crossed the imaginary axis as a complex conjugate pair in the Hopf bifurcation that led to the oscillatory front pattern of Fig. 1(b) and became real as Z increased further. By choosing initial conditions corresponding to the front solution plus or minus a small component in one eigendirection, the unstable directions can be traced out. The result of this procedure is shown in Fig. 4 for $Z = 26.930$. Three of the four initial conditions lead directly to a pulse that travels to the other wall [Figs. 4(a)–4(c)]. The fourth leads to the simultaneous decay of the front at one boundary and growth of a front at the other boundary [Fig. 4(d)]. This motion is essentially one-half cycle of antiphase oscillation. All of these initial conditions evolve into the intermediate pattern of Fig. 2(b). Thus we find that both heteroclinic

FIG. 4. Results of integration in the unstable directions of the stationary front pattern at $Z = 26.930$, in the transition region between back-and-forth and unidirectional motions [cf. Fig. 2(b)], showing that trajectories near the unstable front undergo either antiphase or traveling pulse motions. (a) and (b) integrations in least unstable direction; (c) and (d) integrations in most unstable direction.

paths discussed above are followed, depending on initial conditions.

These nearly heteroclinic paths are the building blocks for the patterns of Fig. 2. Each pattern is essentially a concatenation of such paths and can be represented symbolically. We now see that the left- and right-originating pulses labeled L and R above correspond to one pair of heteroclinic paths. We complete the symbolic description of the dynamics by labeling the two halves of an antiphase oscillation as S and D. One period of the unidirectional motion is a concatenation consisting of a pulse moving from one end of the ribbon to the other, followed by half a period of antiphase oscillation, so the complete symbol sequence is $\overline{LD}$ or $\overline{RS}$. The complete sequence for back-and-forth motion is still $\overline{RL}$, as no antiphase motions are involved. In the transition region, the concatenations are more complex, but S must always be preceded by R and D by L. No sequences with S and D adjacent have been observed.

To better understand this situation, we first consider the special case in which all the paths are *exactly* heteroclinic. This structure is characteristic of the gluing bifurcation [26,27], a codimension-two global bifurcation that occurs when two heteroclinic cycles (or homoclinic orbits, in the absence of symmetry) coincide. Figure 5(a) is a schematic summary of the double heteroclinic phase space structure, showing also the symbols and cartoons of the corresponding spatiotemporal structures. If the parameters are changed slightly, the structure of Fig. 5(a) is perturbed, so that the trajectories are no longer exactly heteroclinic. However, trajectories close to the individual heteroclinic paths can be "glued" together to form periodic or nonperiodic orbits of various degrees of complexity. This gluing process is responsible for the intermediate patterns of Figs. 2(b) and 2(c). Figure 5(b) is the schematic phase diagram showing behavior near the double heteroclinic point in parameter space [26,27]. The unfolding parameters μ_1 and μ_2 are chosen so that $\mu_1 = 0$ and $\mu_2 = 0$ are the loci of the two individual heteroclinic bifurcations. Thus the doubly singular structure of Fig. 5(a) arises at the origin of Fig. 5(b). The crosshatched regions indicate intermediate behavior and in fact contain an infinite number of homoclinic and heteroclinic connections. Our numerical results are consistent with a path through parameter space corresponding to the thick diagonal line. The antiphase motion becomes heteroclinic as the line $\mu_2 = 0$ is crossed and the back-and-forth motion becomes heteroclinic within the transition region, at $\mu_1 = 0$. Note that this unfolding also predicts that a transition from antiphase to unidirectional behavior might be found elsewhere in parameter space. This is observed in numerical simulations [29].

In contrast to the previous transition, during the transition from back-and-forth to unidirectional pulses the instantaneous phase plane characterization changes between B' and O each time a pulse approaches a boundary. Loosely speaking, a sort of "dynamic" saddle-node bifurcation occurs as the low-temperature stable steady state loses existence. Of course this is not actually the case because the current is not a parameter, but a functional of the solution, and because the spatiotemporal dynamics do not occur on the phase plane. Nevertheless, the instantaneous phase plane characteristic is related to the overall behavior of the system. Figure 6 shows the instantaneous nullclines $f = 0$ and $g = 0$ at the highest and lowest current values obtained for the pattern of Fig. 2(b). The "dynamic saddle-node bifurcation" is apparently a necessary condition for the transition, as it allows the ignition of the extinguished region of the domain and thus the birth of a new front (the antiphase motion). Note, however, that in the intermediate region, this dynamic saddle-node bifurcation may occur whenever a pulse approaches a wall, whether the pulse disappears or bounces, so it is not a sufficient condition.

To conclude the discussion of the transitions, Fig. 7 shows a schematic bifurcation diagram, showing all relevant branches. The two boxed regions contain the transitions discussed above, while the remainder of the diagram shows the global branch structure of the solutions that contribute to these transitions. Solid curves are stable

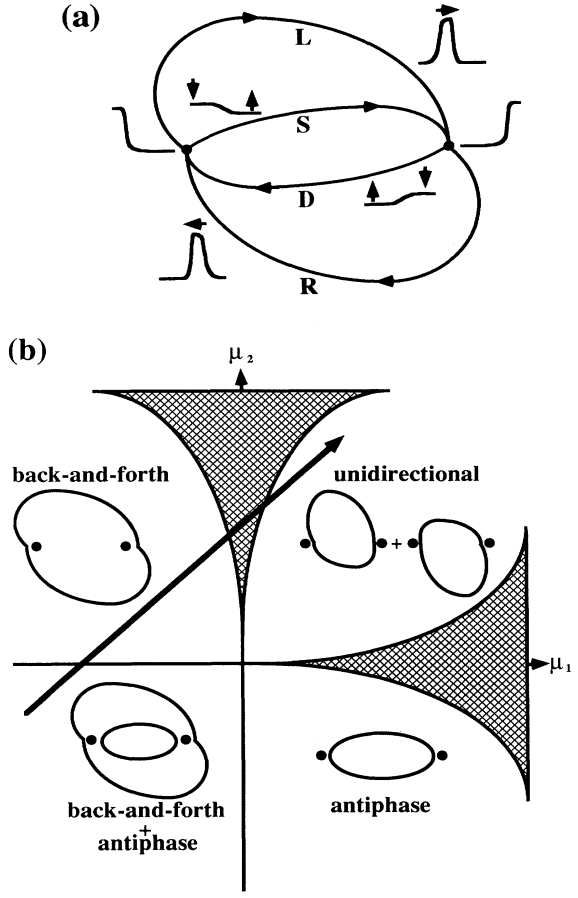

FIG. 5. (a) Schematic global phase-space structure at the gluing bifurcation. (b) Behavior in the parameter space neighborhood of the doubly degenerate structure of (a), which occurs at the origin in this phase diagram. The cross-hatched regions indicate intermediate patterns. The thick diagonal line represents the path through this diagram taken in our system by increasing Z at the parameters chosen.

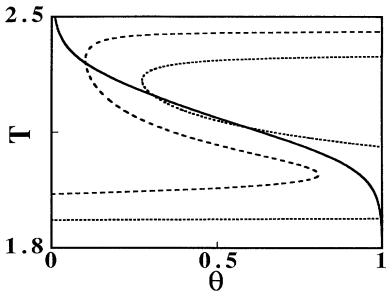

FIG. 6. The nullcline $f = 0$ at the minimum (dotted curve) and maximum (dashed curve) current values during the intermediate motion in Fig. 2(b), $Z = 26.930$. The nullcline $g = 0$, which is independent of current, is also plotted (solid curve), to show the "dynamic saddle-node" behavior associated with the back-and-forth to unidirectional transition.

branches and dashed curves are unstable. The horizontal line at the bottom represents the spatially uniform solution (u). The three branches emanating from it are, from left to right, the antiphase oscillation of wave-number unity (ap1), the stationary front (sf), and the antiphase oscillation of wave number two (ap2). The oscillatory front solution of Fig. 1(b) is labeled (of). The curves labeled bf and ud denote the periodic back-and-forth and unidirectional motions [Figs. 2(a) and 2(d)], respectively. The notations PF, H, and PD denote pitchfork, Hopf, and period-doubling bifurcations, respectively, and PFP denotes a pitchfork bifurcation of a periodic solution. Ho indicates a homoclinic connection and He a heteroclinic one. Corresponding to the Ho and He labels are vertical lines connecting the solutions involved. C is the transition region including the period-doubling cascade, symmetric crisis, and reverse transition to the periodic back-and-forth motion. G denotes the transition region found in the unfolding of the gluing bifurcation [Figs. 2(b) and 2(c)]. Note that the **C** and **G** regions have been greatly oversimplified. There are infinitely many global bifurcations within each of these regions; for simplicity only one was shown for each.

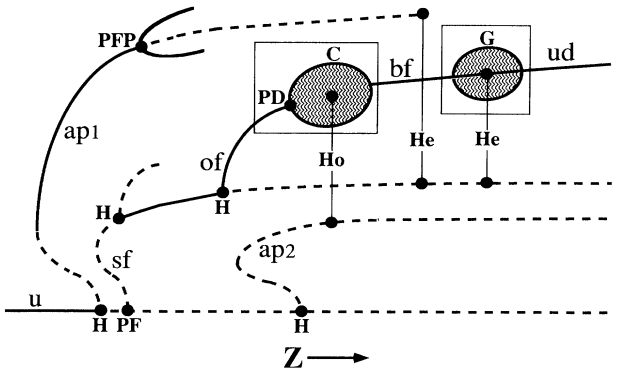

FIG. 7. Schematic bifurcation diagram, showing the solutions that contribute to the global phenomena discussed here. The description of the labels is in the text.

There exist some similarities between the patterns presented here and the "blinking states" found near the onset of binary fluid convection [34,35]. These states exhibit irregular reversals in the directions of traveling wave motions, somewhat like those observed here. An analysis by Dangelmayr and Knobloch shows that these blinking states arise in the unfolding of the Hopf bifurcation in systems with broken circular symmetry (due to distant sidewalls in the case of convection) [36]. A heteroclinic connection occurs in this unfolding and leads to the irregularity of the blinking states. In short, these results share three qualities with the results presented here: a reflection invariant domain, traveling motions, and heteroclinic cycles. However, the convection experiments and the corresponding analysis refer to small amplitude traveling patterns near the initial onset of instabilities. In constrast, the traveling pulses described in the present work are "far from onset" and do not originate as instabilities of a uniform state. Thus they are not accessible by a small amplitude analysis. Furthermore, there are two heteroclinic cycles involved in our back and forth to unidirectional transition, not one. Therefore, although there is a resemblance between the blinking states and the present results, the actual correspondence between the results appears to be rather indirect.

V. THE EFFECT OF NONLOCALITY

The results have been presented and discussed without direct reference to the importance of the spatial nonlocality. The most important property of this effect in the present example is that it is desynchronizing. If one section of the domain ignites, another must extinguish. There are several consequences to this constraint.

(i) Stable traveling pulses can arise at current values for which the unconstrained system is bistable. Both fronts of the pulse must move at the same velocity, because the length of the ignited region cannot change.

(ii) Stationary fronts are stabilized in the absence of diffusion of inhibitor (θ). Desynchronization forces the current to approach the (unique) value that will stabilize a stationary front, again by constraining the width of the ignited region. In contrast, if the current is fixed, stationary fronts are generally structurally unstable when θ does not diffuse.

(iii) Antiphase motions are promoted. The constraint prevents the system from oscillating uniformly, so oscillating portions of the domain are out of phase.

The global phase structure shown above depends intimately on all three of these points and thus on the underlying desynchronizing nonlocal effect. Furthermore, the combination of the integral constraint, the tendency of individual elements to evolve toward either ignited or extinguished states, and the preference of the dynamics for long wavelengths acts to restrict the region of function space in which solutions to this problem are likely to be found. This combination is a possible underlying reason for the wealth of global bifurcations in this system. In other words, under such constraints, it may be that solutions are bound to run into one another. It would

be interesting to see whether more rigorous statements to this effect can be made.

The nonlocality imposed in our model arises from an integral constraint of a dependent variable—a very strong condition. In many of the other examples mentioned above, desynchronizing effects are weaker. The nonlinear current systems where the back-and-forth and unidirectional pulses are observed consist of a spatially distributed medium in series with a simple resistor and (constant) voltage source [6,7]. The spatially distributed medium consists essentially of a continuum of nonlinear elements connected in parallel and diffusively coupled. The voltage drop across the resistor is proportional to the integrated current density in the distributed medium. A local decrease in current density leads to an increase in voltage across the entire distributed medium. The total voltage is directly constrained, but that across the distributed medium is not. A system more closely related physically to the one studied here is a ring of catalytic metal in a well-mixed flow reactor. In this reactor, gas-phase transport is virtually instantaneous, so a decrease in reaction rate at one point on the ring causes an increase in the gas-phase reactant concentration and thus in the reaction rate elsewhere on the ring. Complex pulse motions have been experimentally observed in this system [21].

VI. CONCLUSION

We have described a spatially nonlocal reaction-diffusion model that displays complex and interesting spatiotemporal dynamics. These dynamics can be understood in terms of global bifurcations involving stationary pulses, traveling pulses, and antiphase oscillations. The phase-space framework for the global dynamics is directly related to the desynchronizing nonlocal effect. Such effects also arise in other systems, where some of the behavior analyzed here has been observed experimentally. In addition, the dynamics we observe are, to a degree, independent of the specific form of the nonlinearity, as qualitatively identical transitions also arise in a model with simple polynomial nonlinearities. Thus we believe that the foregoing discussion provides a foundation for analyses of other physical systems with nonlocal effects.

ACKNOWLEDGMENTS

This work was supported by the NSF. The authors thank Martin Golubitsky, Gemunu Gunaratne, Moshe Sheintuch, and Sam Lane for helpful discussions. Computations were performed at the Pittsburgh Supercomputing Center. We thank Edgar Knobloch for a helpful discussion of the similarities between the present results and the blinking states.

* Permanent address: Department of Chemical Engineering, University of Wisconsin, Madison, WI 53706.

[1] P. Coullet and G. Iooss, Phys. Rev. Lett. **64**, 866 (1990).
[2] J. Elezgaray and A. Arneodo, J. Chem. Phys. **95**, 323 (1991).
[3] J. Elezgaray and A. Arneodo, Phys. Rev. Lett. **68**, 714 (1992).
[4] W. Y. Tam and H. L. Swinney, Physica D **46**, 10 (1990).
[5] F. J. Elmer, Physica D **30**, 321 (1988).
[6] C. Radehaus, R. Dohmen, H. Willebrand, and F.-J. Niedernostheide, Phys. Rev. A **42**, 7426 (1990).
[7] H. Willebrand, T. Hüntler, F. J. Niedernostheide, R. Dohmen, and H.-G. Purwins, Phys. Rev. A **45**, 8766 (1992).
[8] G. Ertl, Science **254**, 1750 (1991).
[9] V. Barelko, I. I. Kurochka, A. G. Merzhanov, and K. G. Shkadinskii, Chem. Eng. Sci. **33**, 805 (1978).
[10] V. V. Barelko, V. M. Belbutyan, Yu. E. Volodin, and Ya. B. Zel'dovich, Chem. Eng. Sci. **38**, 1775 (1983).
[11] M. Sheintuch, Chem. Eng. Sci. **44**, 1081 (1989).
[12] G. A. Cordonier, F. Schüth, and L. D. Schmidt, J. Chem. Phys. **91**, 5374 (1989).
[13] G.A. Cordonier and L.D. Schmidt, Chem. Eng. Sci. **44**, 1983 (1989).
[14] L. Lobban, G. Philippou, and D. Luss, J. Phys. Chem. **93**, 733 (1989).
[15] M. Sheintuch, J. Phys. Chem. **94**, 5889 (1990).
[16] G. Philippou, F. Schultz, and D. Luss, J. Phys. Chem. **95**, 3224 (1991).
[17] G. Philippou and D. Luss, J. Phys. Chem. **96**, 6651 (1992).
[18] G. Philippou and D. Luss, Chem. Eng. Sci. **12**, 2313 (1993).
[19] O. Lev, M. Sheintuch, C. Yarnitzky, and L. Pismen, Chem. Eng. Sci. **45**, 839 (1990).
[20] S. L. Lane and D. Luss, Phys. Rev. Lett. **70**, 830 (1993).
[21] M. D. Graham, S. L. Lane, and D. Luss, J. Phys. Chem. **97**, 7564 (1993).
[22] E. Knobloch and J. DeLuca, Nonlinearity **3**, 975 (1990).
[23] B. J. Matkowsky and V. Volpert, Physica D **54**, 203 (1992).
[24] P. Chossat and M. Golubitsky, Physica D **32**, 4236 (1988).
[25] M. Dellnitz, M. Golubitsky, and I. Melbourne, in *Bifurcation and Symmetry: Cross Influence Between Mathematics and Applications,* edited by E. Allgower, K. Böhmer, and M. Golubitsky (Birkhäuser, Basel, 1992).
[26] J.-M. Gambaudo, P. Glendinning, and C. Tresser, C.R. Acad. Sci. Paris, Série I **299**, 711 (1984).
[27] P. Glendinning, in *New Directions in Dynamical Systems,* edited by T. Bedford and J. Swift (Cambridge University Press, Cambridge, 1988).
[28] U. Middya, M. Sheintuch, M. D. Graham, and D. Luss, Physica D **63**, 393 (1993).
[29] U. Middya, M. D. Graham, D. Luss, and M. Sheintuch, J. Chem. Phys. **98**, 2823 (1993).
[30] J. Guckenheimer and P. Holmes, *Nonlinear Oscillations, Dynamical Systems and Bifurcations of Vector Fields,* corrected second printing (Springer, Berlin, 1986).
[31] M. Sheintuch and D. Luss, Chem. Eng. Sci. **42**, 41 (1987).
[32] E. J. Doedel, Prog. Num. **30**, 265 (1981).
[33] H. C. Tuckwell, Science **205**, 493 (1979).
[34] J. Fineberg, E. Moses, and V. Steinberg, Phys. Rev. Lett. **61**, 838 (1988).
[35] P. Kolodner and C. M. Surko, Phys. Rev. Lett. **61**, 842 (1988).
[36] G. Dangelmayr and E. Knobloch, Nonlinearity **4**, 399 (1991).